HHS Public Access

Author manuscript

*Biochemistry*. Author manuscript; available in PMC 2017 March 01.

Published in final edited form as:

*Biochemistry*. 2016 March 1; 55(8): 1179–1186. doi:10.1021/acs.biochem.6b00024.

# The Epimerase and Reductase Activities of Polyketide Synthase Ketoreductase Domains Utilize the Same Conserved Tyrosine and Serine Residues

**Xinqiang Xie**[†,‡], **Ashish Garg**[†,‡], **Adrian T. Keatinge-Clay**[#], **Chaitan Khosla**[§], and **David E. Cane**[*,†]

[†]Department of Chemistry, Box H, Brown University, Providence, Rhode Island 02912-9108

[#]Departments of Molecular Biosciences and Chemistry, The University of Texas at Austin, 1 University Station A5300, Austin, TX 78712-0165

[§]Departments of Chemical Engineering, Chemistry, and Biochemistry, Stanford University, Stanford, California 94305

## Abstract

The role of the conserved active site tyrosine and serine residues in epimerization catalyzed by polyketide synthase ketoreductase (PKS KR) domains has been investigated. Both mutant and wild-type forms of epimerase-active KR domains, including the intrinsically redox-inactive EryKR3$^0$ and PicKR3$^0$ as well as redox-inactive mutants of EryKR1, were incubated with [2-$^2$H]-(2*R*,3*S*)-2-methyl-3-hydroxypentanoyl-SACP ([2-$^2$H]-**2**) and 0.05 equiv of NADP$^+$ in the presence of the redox-active, epimerase-inactive EryKR6 domain. The residual epimerase activity of each mutant was determined by tandem equilibrium isotope exchange, in which the first-order, time-dependent washout of isotope from **2** was monitored by LC-MS-MS with quantitation of the deuterium content of the diagnostic pantetheinate ejection fragment (**4**). Replacement of the active site Tyr or Ser residues, alone or together, significantly reduced the observed epimerase activity of each KR domain with minimal effect on substrate binding. Our results demonstrate that the epimerase and reductase activities of PKS KR domains share a common active site, with both reactions utilizing the same pair of Tyr and Ser residues.

## Graphical Abstract

[*]Author to whom correspondence should be sent: David_Cane@brown.edu.
[‡]These authors contributed equally.

**Author Contributions**

The manuscript was written through contributions of all authors. All authors have given approval to the final version of the manuscript.

Supporting Information. Characterization of mutant proteins. Data for tandem EIX and binding assays. This material is available free of charge via the Internet at http://pubs.acs.org.

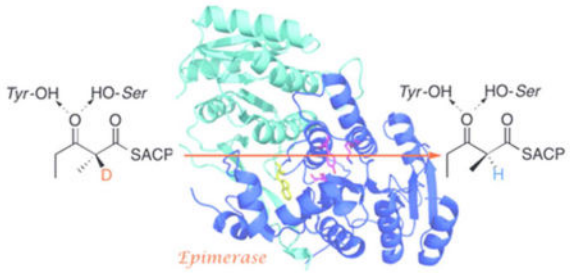


## Introduction

Assembly line polyketide synthases (PKSs) are exceptionally large (1–10 MDa), multifunctional proteins that are responsible for the biosynthesis of a wide range of structurally and stereochemically complex natural products.[1,2] For each PKS, the individual ketoreductase (KR) domains within each module control the configuration of the vast majority of both the secondary hydroxyl and methyl-bearing stereogenic centers in the resultant complex polyketide.[3–13] Thus, EryKR6 from module 6 of the 6-deoxyerythronolide B synthase[14–16] carries out the diastereospecific reduction of its ketosynthase (KS)-generated (2*R*)-2-methyl-3-ketoacyl-acyl carrier protein (ACP) thioester substrate to give (2*R*,3*S*)-2-methyl-3-hydroxyacyl-ACP products (Scheme 1a).[3,4] Using an equilibrium isotope exchange (EIX) assay, we have recently shown that KR domains, such as EryKR1 from module 1 of the 6-deoxyerythronolide B synthase, catalyze mandatory epimerization of the methyl group of the (2*R*)-2-methyl-3-ketoacyl-ACP thioester prior to diastereospecific reduction of the transiently generated (2*S*)-2-methyl-3-ketoacyl-ACP intermediate to give epimerized (2*S*,3*R*)-2-methyl-3-hydroxyacyl-ACP (Scheme 1b).[17] We then used an enzyme-coupled variant assay, termed tandem EIX,[18] to establish that commonly occurring redox-inactive KR domains, such as the EryKR3$^0$ domain from module 3 of the 6-deoxyerythronolide B synthase[16] and the orthologous PicKR3$^0$ domain from module 3 of the picromycin synthase (in which the superscript "$^0$" designates a redox-inactive domain), each harbor an intrinsic, previously cryptic, methyl epimerase activity that generates the (2*S*)-2-methyl-3-ketoacyl-ACP product from the corresponding (2*R*)-2-methyl-3-ketoacyl-ACP intermediate (Scheme 1c).

The overwhelming majority of polyketide synthase KR domains, which all belong to the large and heterogeneous family of short chain dehydrogenase/reductase (SDR) proteins,[19–21] display a universally conserved catalytic triad of Ser, Tyr, and Lys residues (Figure 1). Site-directed mutagenesis of representative PKS KR domains has established that both the Tyr and Ser residues play critical roles in the redox reaction, with the corresponding Tyr→Phe and Ser→Ala mutants retaining <0.1% of the wild-type ketoreductase activity.[22] Extensive biochemical, protein structural, and site-directed mutagenesis studies of prototypical members of the SDR class support a general mechanistic model in which the hydroxyl groups of the active site Tyr and Ser cooperate to hydrogen-bond to the substrate carbonyl oxygen atom, with the phenolic Tyr hydroxyl serving as a general acid that activates the substrate carbonyl for reductive nucleophilic attack by the 4-*si*-hydride of the NADPH cofactor.[23–26]

By contrast, in spite of the apparent mechanistic simplicity of epimerization of a 2-methyl-3-ketoacyl ester, the protein structural basis for the only recently verified intrinsic epimerase activity of specific KR domains has heretofore been obscure. As the next step in addressing this issue, we have now examined the role of the conserved active site Tyr and Ser residues in promoting the discrete KR-catalyzed epimerization event, using an experimental approach that allows deconvolution from the known function of each of these same two residues in catalysis of ketoreductase activity. To this end, we have focused on epimerase-active KR domains such as EryKR3$^0$ and PicKR3$^0$ that are intrinsically redox-inactive, or on engineered variants of EryKR1 that have been rendered redox-inactive as a necessary consequence of mutation of the active site Tyr or Ser residues themselves. The results establish that epimerase and reductase activities of KR domains share a common active site, with the conserved Tyr and Ser residues playing distinct mechanistic roles in promoting each activity.

## Experimental Procedures

### Materials

Isopropylthio-β-galactopyranoside (IPTG), ampicillin, kanamycin, and Phusion Flash High-Fidelity PCR Master Mix were purchased from Thermo Scientific. All other chemical reagents were purchased from Sigma-Aldrich and utilized without further purification. DNA primers were synthesized by Integrated DNA Technologies. Restriction enzymes and T4 DNA ligase were purchased from New England Biolabs Inc (NEB) and used according to the manufacturer's specifications. Competent *E. coli* 10-beta and BL21(DE3) cloning and expression strains were purchased from New England BioLabs. Pre-charged 5 mL HisTrap$^{TM}$ FF columns were purchased from GE Healthcare Life Sciences. Amicon Ultra Centrifugal Filter Units (Amicon Ultra-15 and Amicon Ultra-4, 30,000 MWCO) were purchased from Millipore. Slide-A-Lyzer Dialysis Cassettes was purchased from Thermo Scientific. The black Greiner Bio-One UV-Star® 96-Well Microplates was purchased from VWR Life Science. The construction and sequence information of plasmids containing DNA encoding EryKR1, EryKR3$^0$ and PicKR3$^0$ protein have been previously described.[12,27] Recombinant EryKR1, EryKR3$^0$, PicKR3$^0$, EryKR6, EryACP6 and Sfp were each expressed and purified as previously described.[3,4,12,27,28] The expression and purification of KR mutant proteins is described below. The (±)-2-methyl-3-ketopentanoate-SNAC and propionyl-SNAC were synthesized as previously described.[11] The ACP-bound substrate (2*R*,3*S*)-[2-$^2$H]-2-methyl-3-hydroxypentanoyl-EryACP6 was prepared as previously described.[17,18]

### Methods

General methods were as previously described.[3,29] Growth media and conditions used for *E. coli* strains and standard methods for strain manipulation were as described,[29] unless otherwise noted. All DNA manipulations performed following standard procedures.[29] DNA sequencing was carried out at the U. C. Davis Sequencing Facility, Davis, CA or by Genewiz. All proteins were handled at 4 °C unless otherwise stated. Protein concentrations were determined according to the method of Bradford,[30] using a Tecan Infinite M200 Microplate Reader with bovine serum albumin as the standard. Protein purity and size was

estimated using SDS-PAGE and visualized using Coomassie Blue stain and analyzed with a Bio-Rad ChemiDoc MP System. Accurate protein molecular weight was determined by ESI-MS on an Agilent 6530 Accurate-Mass Q-TOF LC/MS. Reductase activity assays were carried out on the Tecan Microplate Reader and kinetic assays of KR-catalyzed reductions were also performed by GC/MS. $^{1}H$ and $^{13}C$ NMR spectra were obtained on a Bruker Avance III HD Ascend 600 MHz spectrometer. A Thermo LXQ equipped with Surveyor HPLC system and a Phenomenex Jupiter C4 column (150 mm×2 mm, 5.0 μm) was utilized for analysis of diketide-ACP compounds. LC-ESI-MS-MS analysis was carried out in positive ion mode for analysis of pantetheinate ejection fragments.

## KR mutants

Plasmid pAYC59 harboring the DNA sequence encoding the EryKR1 domain[27] served as the template with outside primers (EryKR1-NdeI: 5′-AAAAAACATATGGACGAGGTTTCCGCGCTGCGC-3′, NdeI restriction site underlined; EryKR1-EcoRI: 5′-TTTTGAATTCACCGCGCCCACCCGCGGTTCGGC-3′, EcoRI restriction site underlined) and the corresponding mutant primers (see Table S1) to generate mutations of EryKR1 by two cycles of Overlap Extension PCR.[31] The resultant amplicon was digested with NdeI and EcoRI and ligated into pET28b (Novagen) using the same protocols previously described for preparation of EryKR1 deletion mutants lacking portions of the NADPH binding site.[18] The EryKR3$^{0}$ single mutant was constructed with outside primers (EryKR3- NdeI: 5′-CGAAGTGAACATATGGCGAGCGATGAACTGGCGTACCGC-3′, NdeI restriction site underlined; EryKR3-XhoI: 5′-ATTGCAATGCTCGAGTCAGGCTTCTGCCTGACCCCCGCGGCC-3′, XhoI restriction site underlined) and the corresponding mutant primers (Table S1) using the above protocol. The EryKR3$^{0}$-Y362F mutant plasmid DNA was also used as the template for two further rounds of overlap extension PCR amplification by two pairs of primers (EryKR3-NdeI/XhoI and EryKR3-S349A F/R) to construct the double mutant EryKR3-Y362F/S349A. The same protocol was used to construct the PicKR3$^{0}$ single mutant with outside primers (PicKR3-NdeI: 5′-ATCGTAATCCATATGGGCTCCGTGCAGGACTCCTG-3′, NdeI restriction site underlined; PicKR3-EcoRI: 5′-TGATTCGATGAATTCACGTCGACTGCTGCTCGTCGA-3′, EcoRI restriction site underlined). The PicKR3$^{0}$-Y398F mutant plasmid DNA was also used as the template for two further rounds of overlap extension PCR amplification by two pairs of primers (PicKR3-NdeI/EcoRI and PicKR3-S385A F/R) to construct the double mutant PicKR3$^{0}$-Y398F/S385A. Plasmid DNA was purified (Thermo Scientific GeneJET Plasmid mini-prep kit) in each case from cultures derived from a single colony. DNA sequencing confirmed the sequences of all mutant plasmid inserts.

## Expression and purification of mutant proteins

The expression mutant plasmids were each transformed into competent cells of *E. coli* BL21(DE3) and selected single colonies were inoculated into LB media containing 50 mg/L kanamycin and incubated at 37 °C overnight. The 10-mL seed cultures were each inoculated into 500 mL Super Broth (SB) media containing 50 mg/L kanamycin at 37 °C, which was grown to an $OD_{600}$ of 0.5–0.7. The broth was cooled to 16 °C for 1 h and induced with 0.2

mM ITPG. After 40 h at 16 °C, cells were harvested by centrifugation and washed and resuspended in lysis buffer (50 mM sodium phosphate, 500 mM NaCl, 40 mM imidazole, 10% glycerol, pH 8.0). Following sonication and removal of cell debris by centrifugation (23,000*g* for 50 min), the supernatant was loaded on to a previously lysis buffer-equilibrated, pre-charged 5 mL HisTrapTM FF column (GE Healthcare). The column was washed with 25 mL lysis buffer and then 25 mL washing buffer (50 mM sodium phosphate, 500 mM NaCl, 60 mM imidazole, 10% glycerol, pH 7.6). The protein was eluted using elution buffer (50 mM sodium phosphate, 50 mM NaCl, 150 mM imidazole, 10% glycerol, pH 7.4). The protein was concentrated by ultrafiltration (Amicon, 30,000 MWCO), the buffer was exchanged with exchange buffer (50 mM sodium phosphate, 10% glycerol, pH 7.2), concentrated, and stored at −80 °C until use. SDS-PAGE analysis by Bio-Rad Image Lab Software indicated that the purity of all mutant proteins was >90% and that the relative $M_r$ values were all similar (Figure S2). The molecular mass $M_D$ of each mutant protein was verified by Agilent Technologies Q-TOF LC-MS and matched the predicted values (Table S2).

### Assay of ketoreductase activity of EryKR1-Y370F and EryKR1-S357A mutants

The ketoreductase activity of the EryKR1-Y370F and EryKR1-S357A mutants and wild-type KR proteins was assayed in 96-well plates using the standard assay substrates *trans*-1-decalone and (±)-2-methyl-3-ketopentanoate-S-NAC.[7,32] Each KR protein (5 μM) was incubated with 1 mM NADPH in 50 mM sodium phosphate, pH 7.2, at 30 °C for 20 min. The trans-1-decalone or (±)-2-methyl-3-ketopentanoate-S-NAC (**1**) (final concentration 8.0 mM) was added in a total volume of 200 μL and the consumption of NADPH was measured with the Tecan plate reader by monitoring the decrease in the absorbance at 340 nm for 30 min at 30 °C (Figure S3). The mutant EryKR1-Y370F and EryKR1-S357A proteins did not show any detectable reductase activity in either of these assays.

### GC-MS kinetic assay of EryKR1 and mutant EryKR1-S357A with *trans*-1-decalone

After incubation of EryKR1-Y370F with (±)-2-methyl-3-ketopentanoate-S-NAC or *trans*-1-decalone and NADPH for 24 h, there was no reduced product detected by GC-MS. Under these extended time conditions, the EryKR1-S357A mutant was able to reduce both (±)-2-methyl-3-ketopentanoate-S-NAC or *trans*-1-decalone in the presence of NADPH for 24 h to the corresponding hydroxylated products. EryKR1 (5 μM) or EryKR1-S357A (80 μM) with 2.0 mM NADPH in 50 mM sodium phosphate, pH 7.2 was pre-incubated for 20 min at room temperature, then a concentration series of reference substrate *trans*-1-decalone (final concentration 1, 2, 3, 4, 5, 6, 7, 8 mM) was added and the reaction was quenched by adding 1 mL ethyl acetate after 10 min for EryKR1 (up to 4.5 h) or 6 h for EryKR1-S357A (up to 24 h). The products were extracted with ethyl acetate (3 × 1 mL) and the organic phase was concentrated under vacuum. The residue was resuspended in 200 μL MeOH and then analyzed by GC-MS [Agilent 5977A Series GC/MSD System using HP-5MS capillary column (30 m × 0.25 mm) with the injector port at 250 °C and a temperature program of 60 °C for 2 min, then 20 °C/min up to 280 °C, and 280 °C for 2 min]. A standard calibration curve was generated using *cis*-decahydro-1-naphthol. The steady-state kinetic parameters (Table S3) were calculated by fitting the observed rate and substrate concentration data to

the Michaelis-Menten equation by non-linear least squares regression using the Sigma Plot 12.5 program.

### Tandem equilibrium isotope exchange assay of redox-inactive KR proteins

The tandem EIX assay was based on the previously described protocol, which takes advantage of the fact that EryKR6, EryKR1, EryKR3$^0$, and PicKR3$^0$ are able to process ACP-bound diketide substrates of the appropriate stereochemistry.[18] In a typical assay, [2-$^2$H]-(2*R*,3*S*)-2-methyl-3-hydroxypentanoyl-EryACP6 (**2**) (90 μL of 500 μM solution, 45 nmol, final conc 300 μM), EryKR6 (11.25 nmol, 75 μM), mutant redox-inactive KR protein (11.25 nmol, 75 μM), and $NADP^+$ (1.5 μL of 1.5 mM soln, 2.25 nmol, final conc 15 μM) were incubated in 50 mM phosphate buffer (pH 7.2) (tot vol 150 μL) at room temp. Samples were withdrawn at periodic intervals up to 60 min and frozen in liq $N_2$, before direct analysis of the pantetheinate ejection fragments by LC-ESI(+)-MS-MS, as previously described (Tables S4 and S5).[17,18,33,34]

### Fluorescence quenching assay of (±)-2-methyl-3-ketopentanoyl-SNAC and propionyl-SNAC binding by ketoreductases and mutants

All fluorescence measurements were carried out at pH 7.2 on a Tecan plate reader at 30 °C. Binding of (±)-2-methyl-3-ketopentanoate-SNAC (**1**) to ketoreductases or mutants was monitored by following the quenching of enzyme fluorescence intensity induced by their binding to the NADPH-free apoenzymes.[35,36] Wild type KR domains and their mutant apoenzymes were prepared by previously published methods.[35,36] Purified protein (2 mL) was dialyzed (Slide-A-Lyzer Dialysis Cassettes, 10K MWCO, Thermo Scientific) against 1 L of 50 mM potassium phosphate buffer (pH 7.5) containing 1 M potassium bromide and 5 mM EDTA, 10% glycerol. The buffer was changed two times over a period of 36 h. The dialysis cassettes containing the cofactor-free apoenzyme were then transferred to 2 L of 50 mM sodium phosphate buffer (pH 7.5) containing 10% glycerol with changing of the buffer three times over 36 h. Successive 5-μL portions of substrate (±)-2-methyl-3-ketopentanoyl-SNAC (**1**) solution were added into wells of UV-Star® 96-Well Microplates (Greiner Bio-One, black) containing 90 μL of 1 μM protein solution or buffer alone. The final (±)-2-methyl-3-ketopentanoyl-SNAC concentration in the assay ranged from 0 to 50 mM (0, 0.1, 0.2, 0.4, 1, 1.5, 2, 2.5, 3, 3.5, 4, 10, 15, 20, 25, 30, 35, 40, 45, 50 mM). The plate was incubated for 20 min at room temperature. The quenching fluorescence was excited at 280 nm (5 nm bandwidth) and monitored at 338 nm (20 nm bandwidth). From the measured fluorescence intensity F at a given final concentration of (±)-2-methyl-3-ketopentanoyl-SNAC (Figure S5), the quenched fluorescence intensity $F_q$ was calculated by using the equation $F_q=F_{apo}-F_{obs}$, where the $F_{apo}$ represents the fluorescence intensity of the apoenzyme without (±)-2-methyl-3-ketopentanoyl-SNAC, and $F_{obs}$, the fluorescence intensity of apoenzyme at a given (±)-2-methyl-3-ketopentanoyl-SNAC concentration. The binding parameter ($K_d$) was calculated by fitting the observed quenched fluorescence intensity and substrate concentration data to the Ligand Binding Equation (one site saturation, eq 1) using the SigmaPlot 12.5 program (Table S6).

$$F_q = \frac{\Delta F_{max} * [S]}{K_D + [S]} \quad \text{(Eq 1)}$$

To compare the effect on binding affinity of different substrates, the apoenzyme of EryKR3 and its mutants (Y362F, S349A, Y362F/S349A) were each incubated in separate experiments with (±)-2-methyl-3-ketopentanoyl-SNAC or propionyl-SNAC. The measured fluorescence intensity F at a given final concentration of (±)-2-methyl-3-ketopentanoyl-SNAC or propionyl-S-NAC is shown in Figure S6. The calculated binding affinities ($K_d$) are listed in Table S7. Except for the protein concentration (400 nM) and substrate concentrations (0, 0.75, 4.5, 6, 15, 22.5, 30, 37.5, 45, 52.5, 60, 67.5 mM), all other details of the experiment were the same as those described above. The calculated $K_d$ values for the propionyl-SNAC for each protein variant were 4–7-fold higher than the corresponding values for the (±)-2-methyl-3-ketopentanoyl-SNAC analogue.

## Results

To test the role of the conserved active site Tyr and Ser residues in the epimerase activity of intrinsically epimerase-active KR domains, we first prepared the individual Y362F and S349A mutants as well as the Y362F/S349A double mutant of recombinant EryKR3$^0$ by site-directed mutagenesis. The residual epimerase activity of each redox-inactive EryKR3$^0$ mutant was then determined by enzyme-coupled, tandem EIX assay (Scheme 2).[18] Thus EryKR3$^0$ and each of its mutants were individually incubated with [2-$^2$H]-(2*R*,3*S*)-2-methyl-3-hydroxypentanoyl-SACP ([2-$^2$H]-**2**) and 0.05 equiv of NADP$^+$ in the presence of the redox-active, epimerase-inactive EryKR6 domain (Scheme 2a). EryKR6 serves to transiently generate [2-$^2$H]-(2*R*)-2-methyl-3-ketopentanoyl-ACP (**3**), which can undergo equilibrium isotope exchange catalyzed by any residual epimerase activity in the EryKR3$^0$ mutant. Under these equilibration conditions, **3** is reduced back to **2** by EryKR6 using the transiently generated NADPH. The extent of first-order, time-dependent net washout of isotope from **2** was monitored by LC-MS-MS analysis of samples withdrawn at periodic intervals over a period of an hour, with quantitation of the deuterium content of the diagnostic pantetheinate ejection fragment **4** derived from **2** (Scheme 2c, Figures 2a and 3, Table S4).[33,34] As positive and negative controls, incubations were also carried out with wild-type EryKR3$^0$ (Scheme 2a, Figure 2a, Table S4) and with EryKR6 alone (Scheme 2b, Figure 2a, Table S4), respectively, in order to establish the upper and lower limits of KR-catalyzed deuterium exchange. The relative rate of deuterium washout for each mutant compared to the rate for epimerase-active wild-type EryKR3$^0$ was then calculated from the ratio of the slopes of the first-order fits of ln(%$^2$H) of **2** vs time from 20 – 60 min, after correction for the small amount of background exchange measured in the presence of epimerase-inactive EryKR6 alone (Table S5). By this method, it was found that the Y362F and S349A mutants of EryKR3$^0$ each lost >85% of their native epimerase activity, while the Y362F/S349A double mutant lost >95% of the original epimerase activity, with the measured washout of deuterium from [2-$^2$H]-**2** being essentially indistinguishable from the background loss of isotope observed with EryKR6 alone (Figures 2a and 3, Tables S4 and S5). Significantly, both the S349A and Y362F/S349A mutants also displayed lag times of at least 30 min before the onset of detectable loss of deuterium, as typically observed in the

EIX assay of epimerase-inactive KR domains such as EryKR6 (Figures 2a and 3, Table S4).[17,18]

As a further control, the dissociation constants $K_d$ for wild-type EryKR3$^0$ and for the three derived mutants were determined by titration of each protein with the substrate analogue (±)-2-methyl-3-ketopentanoyl-*N*-acetycysteamine (SNAC) thioester (**1**) and measurement of the resultant protein fluorescence quenching (Figure S5 and Table S6).[35,36] The $K_d$ value for the diketide-SNAC ester was analyzed rather than that of the corresponding ACP-tethered thioester **3** in order to focus on the effect of the individual KR mutations on binding of the 2-methyl-3-ketoacyl diketide moiety, without masking by the stronger binding of the ACP moiety. ACP-bound substrates typically exhibit $K_m$ values that are about 0.1% of those for the corresponding SNAC analogues, presumably due to substantial protein-protein interactions between the KR domain and the ACP itself. As a further validation of the binding assay itself, we also tested the non-reactive substrate analogue propionyl-SNAC, which showed $K_d$ values for EryKR3$^0$ and its mutants that were 4–7-fold larger than those for the diketide analogue 2-methyl-3-ketopentanoyl-SNAC (Figure S6 and Table S7). Notably the calculated $K_d$ values for diketide-SNAC **1** with each of the three mutants increased by no more than 15% from the $K_d$ of 8.0±0.4 mM determined for wild-type EryKR3$^0$, thereby establishing that neither of these two mutations, alone or together, significantly affected the binding of the 2-methyl-3-ketoacyl thioester substrate. The steady-state parameters $k_{cat}$ and $K_m$ of the actual epimerase substrate, 2-methyl-3-ketopentanoyl-SACP (**3**) can of course not be measured under the conditions of the tandem EIX assay, since the actual concentration of **3** that is transiently generated in the enzyme-coupled reaction is necessarily indeterminate.

To probe the generality of these observations, we also carried out an analogous series of experiments (Scheme 2) on the corresponding Y398F, S385A, and Y398F/S385A mutants of the intrinsically epimerase-active PicKR3$^0$ domain, with results similar to those observed for the EryKR3$^0$ mutant series (Figures 2b and S4, Tables S4 and S5). While replacement of the Tyr residue with Phe resulted in a modest 44% decrease in epimerase activity, the Ser→Ala mutation reduced the net epimerase activity by 63%, and the Y398F/S385A double mutant lost essentially all measurable epimerase activity. Control substrate binding assays once again confirmed that the individual mutations resulted in only minor increases in $K_d$ for (±)-2-methyl-3-ketopentanoyl-SNAC (**1**) compared to the $K_D$ of 5.0±0.3 mM for binding of **1** to wild-type PicKR3$^0$ (Figure S5 and Table S6).

In a third series of experiments, we generated the redox-inactive Y370F and S357A mutants of epimerase-active recombinant EryKR1. Both UV spectrometric and GC-MS assays using the model substrates *trans*-1-decalone and (±)-2-methyl-3-ketopentanoyl-SNAC) in the presence of NADPH confirmed the expected near complete abolition of ketoreductase activity in both mutants, with $k_{cat}(mut)/k_{cat}(wt) < 10^{-4}$. (Figure S3, Table S3).[7,32] By contrast, neither mutation had a significant effect on the binding affinity of **1**, with the $K_d$ for both the Y370F and S357A mutants within 20% of the $K_d$ of 7.7±0.4 mM determined for wild-type EryKR1 (Table S6). Using the tandem EIX assay, both the EryKR1 Y370F and S357A mutants exhibited >95% loss in epimerase activity, as well as lag times of 20–30 min

for the onset of detectable deuterium washout typical of epimerase-inactive KR domains (Scheme 2, Figure 2c, Table S4).[17,18]

## Discussion

The above-described experiments establish that the epimerase and reductase activities of PKS KR domains share a common active site and that both reactions utilize the same pair of conserved tyrosine and serine residues. Since the majority of PKS KR domains catalyze only ketoreduction without coupled epimerization, it is evident that the conserved Tyr and Ser residues alone are not sufficient for epimerase activity. Notably, for KR domains such as EryKR1 that are both redox- and epimerase-active, mutation of either the Tyr or Ser residue results in a considerably stronger suppression of ketoreductase activity than of epimerase activity. This differential influence on catalysis is consistent with the substantial differences between the rates of enzyme-catalyzed NADPH-dependent ketoreductase reactions and those reported for NAD(P)H model reactions ($k_{cat}/k_{uncat}$ >$10^6$).[37] These rate accelerations, corresponding to selective stabilization of the enzyme-bound transition state, are at least 3 orders of magnitude larger than the relatively small $k_{cat}/k_{uncat}$ ~1–5 × $10^3$ at pH 7.2 that has been assigned for epimerization of 2-methyl-3-ketoacyl-ACP substrates.[3,4]

We propose that the active site Tyr and Ser residues of an epimerase-active PKS KR domain both hydrogen-bond to the ketone carbonyl of the (2*R*)-2-methyl-3-ketoacyl-ACP substrate, which is thereby held in an extended conformation in which the ketone and thioester carbonyl groups are coplanar, resulting in a $pK_a$ 10–11 for the H-2 proton of the conformationally restricted 3-ketoacyl thioester (Scheme 3). Removal of the H-2 proton by an as yet unidentified basic amino acid residue or a bound water molecule will generate the corresponding conjugated enolate, itself more strongly hydrogen-bonded to the tyrosine and serine hydroxyl groups. Reprotonation at C-2 on the opposite face of the transiently generated enolate by an acidic amino acid residue or a second water molecule will generate the epimerized (2*S*)-2-methyl-3-ketoacyl-ACP. Although to date there are no structures of PKS KR domains with bound substrates, the proposed mode of interaction of the 2-methyl-3-ketoacyl-ACP with the active site Tyr and Ser residues is supported by the combined results of docking experiments and molecular dynamics simulations.[38–40] Intriguingly, neither extensive sequence alignments nor crystal structures of both epimerase-active and epimerase-inactive KR domains have so far revealed any plausible acidic or basic amino acid residues suitably positioned within the active sites to mediate deprotonation or reprotonation at C-2 of the epimerizable substrate.[8–13,38–40] We have previously ruled out any role for the NADPH cofactor in the epimerization reaction itself.[18] Why some KR domains have epimerase activity and some do not is an essential question whose answer remains to be established.

For KR domains such as EryKR1 that are both epimerase- and redox-active, the (2*S*)-2-methyl-3-ketoacyl-ACP intermediate undergoes diastereospecific KR-catalyzed reduction before release from the active site, thereby effecting a net kinetic resolution. By contrast, for epimerase-active, redox-inactive KR domains such as EryKR3$^0$ and PicKR3$^0$, the KS domain of the proximal downstream PKS module is responsible for the kinetic resolution step. For example, we have shown that the NanKS2 domain from module 2 of the

nanchangmycin PKS is strictly diastereospecific for elongation of its natural (2*S*)-2-methyl-3-ketobutyryl-SACP substrate.[41]

Current efforts to elucidate further the mechanism of epimerase-active KR domains are now directed at determination of the structures of KR domains with bound substrates, as well as identification of the crucial active site basic and acidic species that mediate the requisite formation and further reaction of the transient enolate thioester intermediate.

## Supplementary Material

Refer to Web version on PubMed Central for supplementary material.

## Acknowledgments

**Funding Sources**

This work was supported by grants from the U. S. National Institutes of Health, GM022172 to D.E.C., GM106112 to A.K.-C., and GM 087934 to C.K. and Welch Foundation grant F-1712 to A.K.-C.

## Abbreviations

| | |
|---|---|
| **ACP** | acyl carrier protein |
| **EIX** | equilibrium isotope exchange |
| **ESI** | electrospray ionization |
| **KR** | ketoreductase |
| **GC-MS** | gas chromatography-mass spectrometry |
| **IPTG** | isopropylthio-β-galactopyranoside |
| **KS** | ketosynthase |
| **LC-MS** | liquid chromatography-mass spectrometry |
| **PKS** | polyketide synthase |
| **SDR** | short chain dehydrogenase/reductase |
| **SNAC** | *N*-acetylcysteamine |

## References

1. Hopwood, DA. Complex enzymes in microbial natural product biosynthesis, part B: polyketides, aminocoumarins and carbohydrates. Vol. 459. Academic Press; 2009. Methods in Enzymology.
2. Khosla C, Tang Y, Chen AY, Schnarr NA, Cane DE. Structure and mechanism of the 6-deoxyerythronolide B synthase. Annu Rev Biochem. 2007; 76:195–221. [PubMed: 17328673]
3. Valenzano CR, Lawson RJ, Chen AY, Khosla C, Cane DE. The biochemical basis for stereochemical control in polyketide biosynthesis. J Am Chem Soc. 2009; 131:18501–18511. [PubMed: 19928853]
4. Castonguay R, He W, Chen AY, Khosla C, Cane DE. Stereospecificity of ketoreductase domains of the 6-deoxyerythronolide B synthase. J Am Chem Soc. 2007; 129:13758–13769. [PubMed: 17918944]

5. Castonguay R, Valenzano CR, Chen AY, Keatinge-Clay A, Khosla C, Cane DE. Stereospecificity of ketoreductase domains 1 and 2 of the tylactone modular polyketide synthase. J Am Chem Soc. 2008; 130:11598–11599. [PubMed: 18693734]
6. You YO, Khosla C, Cane DE. Stereochemistry of reductions catalyzed by methyl-epimerizing ketoreductase domains of polyketide synthases. J Am Chem Soc. 2013; 135:7406–7409. [PubMed: 23659177]
7. Siskos AP, Baerga-Ortiz A, Bali S, Stein V, Mamdani H, Spiteller D, Popovic B, Spencer JB, Staunton J, Weissman KJ, Leadlay PF. Molecular basis of Celmer's rules: stereochemistry of catalysis by isolated ketoreductase domains from modular polyketide synthases. Chem Biol. 2005; 12:1145–1153. [PubMed: 16242657]
8. Keatinge-Clay AT, Stroud RM. The structure of a ketoreductase determines the organization of the beta-carbon processing enzymes of modular polyketide synthases. Structure. 2006; 14:737–748. [PubMed: 16564177]
9. Keatinge-Clay AT. A tylosin ketoreductase reveals how chirality is determined in polyketides. Chem Biol. 2007; 14:898–908. [PubMed: 17719489]
10. Zheng J, Taylor CA, Piasecki SK, Keatinge-Clay AT. Structural and functional analysis of A-Type ketoreductases from the amphotericin modular polyketide synthase. Structure. 2010; 18:913–922. [PubMed: 20696392]
11. Piasecki SK, Taylor CA, Detelich JF, Liu J, Zheng J, Komsoukaniants A, Siegel DR, Keatinge-Clay AT. Employing modular polyketide synthase ketoreductases as biocatalysts in the preparative chemoenzymatic syntheses of diketide chiral building blocks. Chem Biol. 2011; 18:1331–1340. [PubMed: 22035802]
12. Zheng J, Keatinge-Clay A. Structural and functional analysis of C2-type ketoreductases from modular polyketide synthases. J Mol Biol. 2011; 410:105–117. [PubMed: 21570406]
13. Zheng J, Piasecki SK, Keatinge-Clay AT. Structural studies of an A2-type modular polyketide synthase ketoreductase reveal features controlling alpha-substituent stereochemistry. ACS Chem Biol. 2013; 8:1964–1971. [PubMed: 23755878]
14. Cortes J, Haydock SF, Roberts GA, Bevitt DJ, Leadlay PF. An unusually large multifunctional polypeptide in the erythromycin-producing polyketide synthase of *Saccharopolyspora erythraea*. Nature. 1990; 348:176–178. [PubMed: 2234082]
15. Donadio S, Staver MJ, Mcalpine JB, Swanson SJ, Katz L. Modular organization of genes required for complex polyketide biosynthesis. Science. 1991; 252:675–679. [PubMed: 2024119]
16. Donadio S, Katz L. Organization of the enzymatic domains in the multifunctional polyketide synthase involved in erythromycin formation in *Saccharopolysporaerythraea*. Gene. 1992; 111:51–60. [PubMed: 1547954]
17. Garg A, Khosla C, Cane DE. Coupled methyl group epimerization and reduction by polyketide synthase ketoreductase domains. Ketoreductase-catalyzed equilibrium isotope exchange. J Am Chem Soc. 2013; 135:16324–16327. [PubMed: 24161343]
18. Garg A, Xie X, Keatinge-Clay A, Khosla C, Cane DE. Elucidation of the cryptic epimerase activity of redox-inactive ketoreductase domains from modular polyketide synthases by tandem equilibrium isotope exchange. J Am Chem Soc. 2014; 136:10190–10193. [PubMed: 25004372]
19. Kallberg Y, Oppermann U, Jornvall H, Persson B. Short-chain dehydrogenases/reductases (SDRs). Eur J Biochem. 2002; 269:4409–4417. [PubMed: 12230552]
20. Kallberg Y, Oppermann U, Jornvall H, Persson B. Short-chain dehydrogenase/reductase (SDR) relationships: a large family with eight clusters common to human, animal, and plant genomes. Protein Sci. 2002; 11:636–641. [PubMed: 11847285]
21. Oppermann U, Filling C, Hult M, Shafqat N, Wu X, Lindh M, Shafqat J, Nordling E, Kallberg Y, Persson B, Jornvall H. Short-chain dehydrogenases/reductases (SDR): the 2002 update. Chem Biol Interact. 2003; 143–144:247–253.
22. Reid R, Piagentini M, Rodriguez E, Ashley G, Viswanathan N, Carney J, Santi DV, Hutchinson CR, McDaniel R. A model of structure and catalysis for ketoreductase domains in modular polyketide synthases. Biochemistry. 2003; 42:72–79. [PubMed: 12515540]

23. Liu Y, Thoden JB, Kim J, Berger E, Gulick AM, Ruzicka FJ, Holden HM, Frey PA. Mechanistic roles of tyrosine 149 and serine 124 in UDP-galactose 4-epimerase from *Escherichia coli*. Biochemistry. 1997; 36:10675–10684. [PubMed: 9271498]
24. Hardwicke MA, Rendina AR, Williams SP, Moore ML, Wang L, Krueger JA, Plant RN, Totoritis RD, Zhang G, Briand J, Burkhart WA, Brown KK, Parrish CA. A human fatty acid synthase inhibitor binds beta-ketoacyl reductase in the ketosubstrate site. Nat Chem Biol. 2014; 10:774–779. [PubMed: 25086508]
25. Thoden JB, Hegeman AD, Wesenberg G, Chapeau MC, Frey PA, Holden HM. Structural analysis of UDP-sugar binding to UDP-galactose 4-epimerase from *Escherichia coli*. Biochemistry. 1997; 36:6294–6304. [PubMed: 9174344]
26. Thoden JB, Frey PA, Holden HM. Molecular structure of the NADH/UDP-glucose abortive complex of UDP-galactose 4-epimerase from *Escherichia coli*: implications for the catalytic mechanism. Biochemistry. 1996; 35:5137–5144. [PubMed: 8611497]
27. Chen AY, Cane DE, Khosla C. Structure-based dissociation of a type I polyketide synthase module. Chem Biol. 2007; 14:784–792. [PubMed: 17656315]
28. Chen AY, Schnarr NA, Kim CY, Cane DE, Khosla C. Extender unit and acyl carrier protein specificity of ketosynthase domains of the 6-deoxyerythronolide B synthase. J Am Chem Soc. 2006; 128:3067–3074. [PubMed: 16506788]
29. Sambrook, J.; Fritsch, EF.; Maniatis, T. Molecular Cloning, A Laboratory Manual. 2. Cold Spring Harbor Laboratory Press; Cold Spring Harbor, NY: 1989.
30. Bradford M. A rapid and sensitive method for the quantitation of microgram quantitites of protein utilizing the principle of protein-dye binding. Anal Biochem. 1976; 72:248–254. [PubMed: 942051]
31. Bryksin AV, Matsumura I. Overlap extension PCR cloning: a simple and reliable way to create recombinant plasmids. Biotechniques. 2010; 48:463–465. [PubMed: 20569222]
32. Wong H, Mattick JS, Wakil SJ. The architecture of the animal fatty acid synthetase. III Isolation and characterization of β-ketoacyl reductase. J Biol Chem. 1983; 258:15305–15311. [PubMed: 6361031]
33. Dorrestein PC, Bumpus SB, Calderone CT, Garneau-Tsodikova S, Aron ZD, Straight PD, Kolter R, Walsh CT, Kelleher NL. Facile detection of acyl and peptidyl intermediates on thiotemplate carrier domains via phosphopantetheinyl elimination reactions during tandem mass spectrometry. Biochemistry. 2006; 45:12756–12766. [PubMed: 17042494]
34. Meluzzi D, Zheng WH, Hensler M, Nizet V, Dorrestein PC. Top-down mass spectrometry on low-resolution instruments: characterization of phosphopantetheinylated carrier domains in polyketide and non-ribosomal biosynthetic pathways. Bioorg Med Chem Lett. 2008; 18:3107–3111. [PubMed: 18006314]
35. He XM, Thorson JS, Liu HW. Probing the coenzyme and substrate binding events of CDP-D-glucose 4,6-dehydratase: Mechanistic implications. Biochemistry. 1996; 35:4721–4731. [PubMed: 8664262]
36. Menon S, Stahl M, Kumar R, Xu GY, Sullivan F. Stereochemical course and steady state mechanism of the reaction catalyzed by the GDP-fucose synthetase from Escherichia coli. J Biol Chem. 1999; 274:26743–26750. [PubMed: 10480878]
37. He G-X, Blasko A, Bruice TC. $^{1}$H NMR study of the rates and isotope effects of the NADH model hydride transfer reaction. Bioorganic Chem. 1993; 21:423–430.
38. Bailey CB, Pasman ME, Keatinge-Clay AT. Substrate structure-activity relationships guide rational engineering of modular polyketide synthase ketoreductases. Chem Commun. 2015; 52:792–795.
39. Keatinge-Clay AT. Stereocontrol within polyketide assembly lines. Nat Prod Rep. 2016; 33:141–149. [PubMed: 26584443]
40. Mugnai ML, Shi Y, Keatinge-Clay AT, Elber R. Molecular dynamics studies of modular polyketide synthase ketoreductase stereospecificity. Biochemistry. 2015; 54:2346–2359. [PubMed: 25835227]

41. Guo X, Liu T, Deng Z, Cane DE. Essential role of the donor acyl carrier protein in stereoselective chain translocation to a fully reducing module of the nanchangmycin polyketide synthase. Biochemistry. 2012; 51:879–887. [PubMed: 22229794]


**Figure 1.**

Mega3.0 (http://www.megasoftware.net) sequence alignment of epimerase-active PKS KR domains. PKS: Amp, amphotericin; Ery, erythromycin; Lan, lankamycin; Nys, nystatin; Pic, picromycin; Rif, rifamycin.

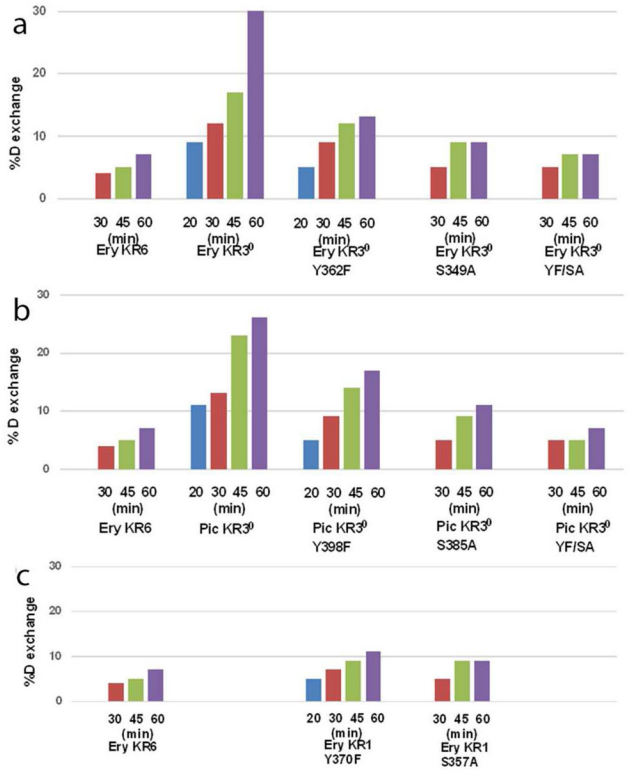


**Figure 2.**

Tandem EIX Assay of washout of deuterium from [2-$^{2}$H]-**2** by redox-inactive KR$^{0}$ domains and derived Tyr and Ser Mutants. a. EryKR3$^{0}$. b. PicKR3$^{0}$. c. EryKR1 mutants.

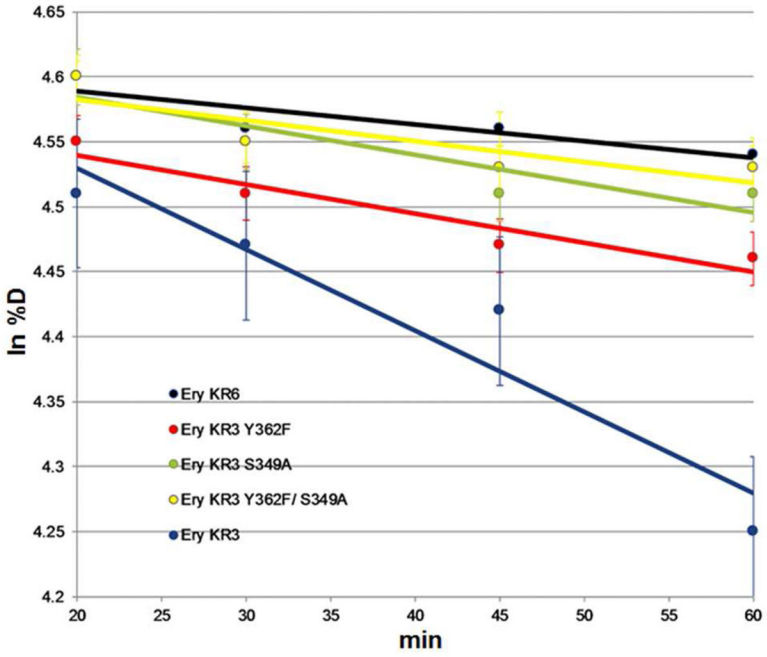


**Figure 3.**

Time-dependent tandem EIX washout of deuterium from [2-$^{2}$H]-**2** by wild-type EryKR3$^{0}$ and mutants.

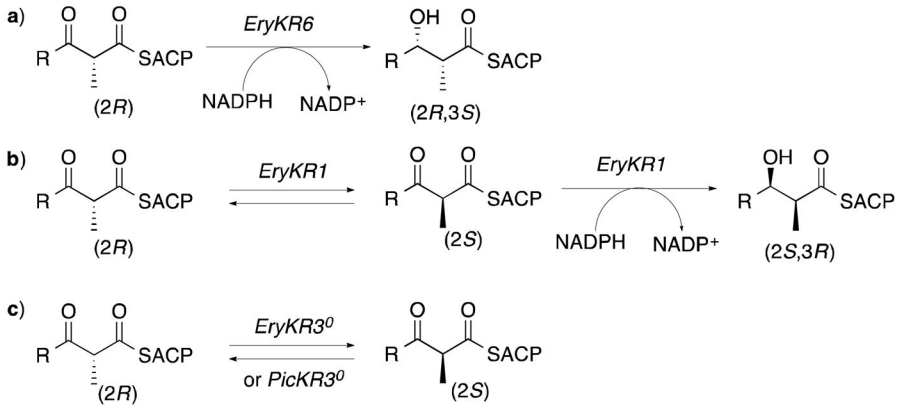


**Scheme 1.**

Epimerase-active and epimerase-inactive KR domains.

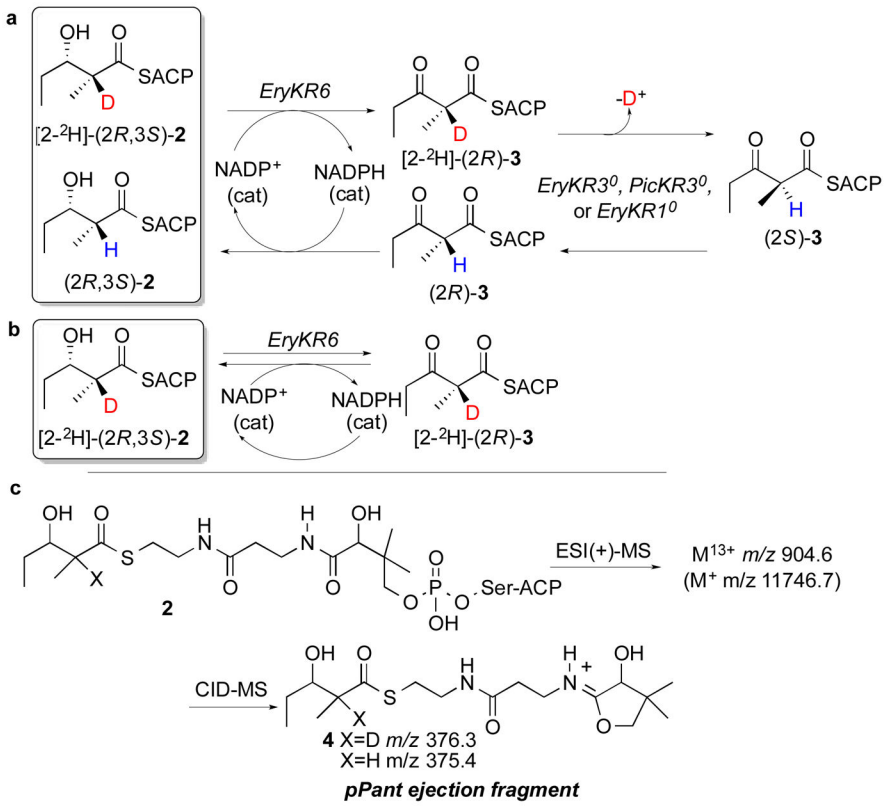


**Scheme 2.**

Tandem EIX assay of epimerase activity of redox-inactive, wild-type and mutant $KR^0$ domains.

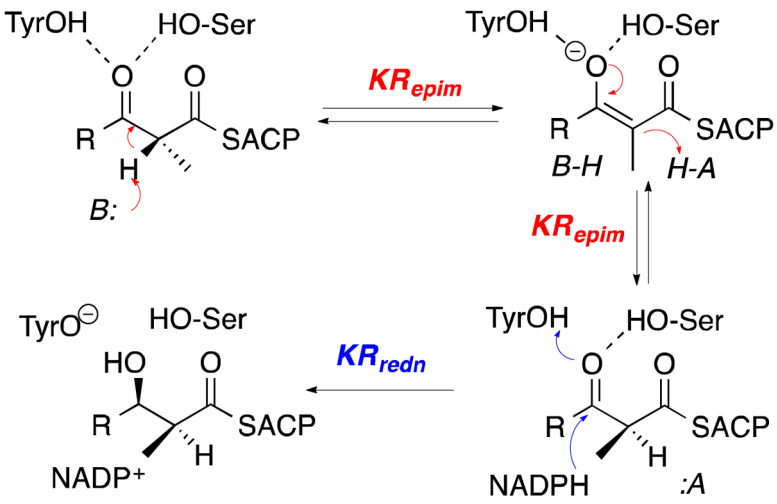


**Scheme 3.**
Proposed mechanism of epimerization - reduction